Journal of Science and Technology in Civil Engineering, HUCE, 2026, 20 (2): 33–47

BUCKLING ANALYSIS FOR PLATES USING FINITE STRIP METHOD BASED ON REFINED MINDLIN–REISSNER PLATE THEORY

Cuong Hung Bui[a], Quoc Dang Tu Chiem[a,b,*], Son Tung Vy[a,c], Andy Nguyen[d]

[a]*Faculty of Civil and Industrial Construction, Hanoi University of Civil Engineering, 55 Giai Phong road, Bach Mai ward, Hanoi, Vietnam*
[b]*Consultancy Company Limited of University of Civil Engineering, 55 Giai Phong road, Bach Mai ward, Hanoi, Vietnam*
[c]*School of Civil and Environmental Engineering, Queensland University of Technology, Australia*
[d]*School of Science, Engineering and Digital Technologies, University of Southern Queensland, Australia*

Article history:
Received 16/12/2025, Revised 17/3/2026, Accepted 13/4/2026

Abstract

This paper presents a three-nodal-line finite strip formulation based on the refined first-order shear deformation plate theory (RFSDT) for the buckling analysis of both thin and thick plates. The proposed finite strip model incorporates the effects of transverse shear deformation, which leads to a significant reduction in the critical buckling stress of plates. Closed-form expressions for the strip stiffness and geometric stiffness matrices are derived using the principle of minimum total potential energy. These matrices enable more efficient structural stress analysis while reducing computational cost. The buckling problem is formulated as an eigenvalue problem obtained from the assembled strip stiffness and geometric stiffness matrices, from which the critical buckling load factors are determined. The results obtained using the proposed finite strip are validated through comparisons with exact solutions and previously published studies. Furthermore, based on an extensive parametric study, practical formulas are proposed for predicting the critical buckling stress of isotropic simply supported plates subjected to uniaxial compression and in-plane bending. The proposed formulas exhibit high reliability, as indicated by low coefficients of variation and high coefficients of determination.

Keywords: finite strip method; buckling analysis; thin plates; thick plates; refined first-order shear deformation plate theory.

https://doi.org/10.31814/stce.huce2026-20(2)-03

1. Introduction

The semi-analytical finite strip method (SAFSM) originally developed by Cheung [1]. This method employs harmonic functions in the longitudinal axis and polynomial functions in the transverse axis. Compared with the finite element method (FEM), the SAFSM requires fewer elements, thereby declining the structural analysis time. Hancock [2] proposed a signature curve to represent local and distortional buckling, thereby assisting engineers in gaining a clearer understanding of the buckling characteristics of cross-sections. SAFSM has been widely employed for the analysis of structural behavior, including bending [3], buckling [4], post-buckling [5], and vibration [6]. Subsequently, this method has also been utilized to investigate the buckling behavior of non-coplanar structures [7] and bridge structures [8]. THIN-WALL program [9] and CUFSM program [10] were developed based on SAFSM, which is formulated on classical plate theory (CPT), to analyze the buckling behavior of sections. Hancock and Pham employed the SAFSM to investigate the shear

*Corresponding author. *E-mail address:* 9241114@st.huce.edu.vn (Chiem, Q. D. T.)

loading [11] and localized loading [12]. A number of studies have successfully incorporated first- and higher-order shear deformation plate theories into the SAFSM to highlight the influence of transverse shear deformation components on the critical buckling stress of moderately thick plates [13], as well as on the behavior of a channel section with intermediate stiffeners in the web [14]. In addition, the behavior of composite plates has also been examined within the framework of the SAFSM by several authors [15–18]. Bui and Chiem explored buckling behavior of thin- and thick-walled open sections [19] and circular hollow sections [20] using higher-order shear deformation plate theories (HSDT). In their publication, classification thin and thick walled members is proposed based on the b/t and D/t for several engineering fields according to local buckling criteria. In addition, formula for determining the critical buckling stress of thin- and thick-walled tubes are also provided.

The refined first-order shear deformation plate theory (RFSDT) is established based on the assumption that the displacement field can be decomposed into bending and shear components [21]. This theory has been widely used in the analysis of plate structures [22–25]. Numerous researchers have incorporated the RFSDT into the semi-analytical finite strip method (SAFSM) to investigate the bending behavior of composite plates [26], buckling behavior [27], and the buckling and vibration of nanoplates [28]. In most of these studies, the displacement field is divided into bending and shear parts, and a third-order polynomial function is adopted for the shear component in order to satisfy the shear stress-free boundary conditions on the top and bottom surfaces of the plate [29]. The RFSDT has also been successfully employed to analyze the static response and free vibration of composite plates [30].

The critical buckling stress of simply supported plates subjected to uniaxial compression and in-plane bending admits exact solution for thin plates [31], 3D elastic [32], Navier solution based on TSDT [33], FEM [34], differential quadrature solution [35], Navier and Levy solutions found on TSDT [36]. Several researchers have proposed formulas for determining the critical buckling stress of thin-walled sections [37–40]. However, although numerous formulas have been developed for predicting the critical buckling stress of plates and structural sections, approximate formulas applicable to thick plates have not yet been established.

As mentioned above, most existing SAFSM formulations have employed refined higher-order shear deformation theories, whereas the incorporation of the refined first-order shear deformation theory (RFSDT) has not yet been fully addressed. In addition, to the best of the authors' knowledge, closed-form solutions for the stiffness matrices have not been provided in previous publications. For the purpose of improving computational efficiency and facilitating practical implementation in structural analysis, closed-form solutions can significantly reduce computational cost and resource requirements. In this study, explicit closed-form stiffness matrices within the SAFSM framework based on the RFSDT are developed to analyze the buckling behavior of both thin and thick plates subjected to uniaxial compression and in-plane bending. The influence of plate thickness on the critical buckling stress is also highlighted through a series of numerical investigations. Furthermore, based on a parametric study, practical formulas are proposed for predicting the critical buckling stress of isotropic simply supported plates under uniaxial compression and in-plane bending.

2. Finite strip solution

2.1. Displacement–strain relation

The displacement field based on the refined first-order shear deformation plate theory (RFSDT) is expressed as follows:

$$\begin{aligned} u(x,y,z) &= u_0(x,y) + z\theta_y(x,y) \\ v(x,y,z) &= v_0(x,y) + z\theta_x(x,y) \\ w(x,y,z) &= w(x,y) \end{aligned} \tag{1}$$

where $u,\ v,\ w,\ \theta_y, \theta_x$ are five displacement components defined on the mid-plane of the plate. Based on the concept of decomposing the transverse deflection into two components, the total deflection is expressed as the sum of the bending deflection w_b and the shear deflection w_s. In addition, by incorporating the assumptions regarding the differential relationship between the rotations and the bending deflection, $\theta_y = -\dfrac{\partial w_b}{\partial x}$, $\theta_x = -\dfrac{\partial w_b}{\partial y}$, the displacement field of RFSDT [30] can be rewritten as follows:

$$\begin{aligned} u(x,y,z) &= u_0(x,y) - z\frac{\partial w_b}{\partial x} \\ v(x,y,z) &= v_0(x,y) - z\frac{\partial w_b}{\partial y} \\ w(x,y,z) &= w_b(x,y) + w_s(x,y) \end{aligned} \tag{2}$$

It can be observed that Eq. (2) involves only four unknown displacement components u_0, v_0, w_b, w_s (see Fig. 1(a)). Accordingly, the strain field based on the RFSDT can be expressed in terms of these four unknown displacements as follows:

$$\begin{aligned} \varepsilon_x &= \frac{\partial u_0}{\partial x} - z\frac{\partial^2 w_b}{\partial x^2}; \quad \varepsilon_y = \frac{\partial v_0}{\partial y} - z\frac{\partial^2 w_b}{\partial y^2} \\ \gamma_{xy} &= \frac{\partial u_0}{\partial y} + \frac{\partial v_0}{\partial x} - 2z\frac{\partial^2 w_b}{\partial x \partial y} \\ \gamma_{xz} &= \frac{\partial w_s}{\partial x}; \quad \gamma_{yz} = \frac{\partial w_s}{\partial y} \end{aligned} \tag{3}$$

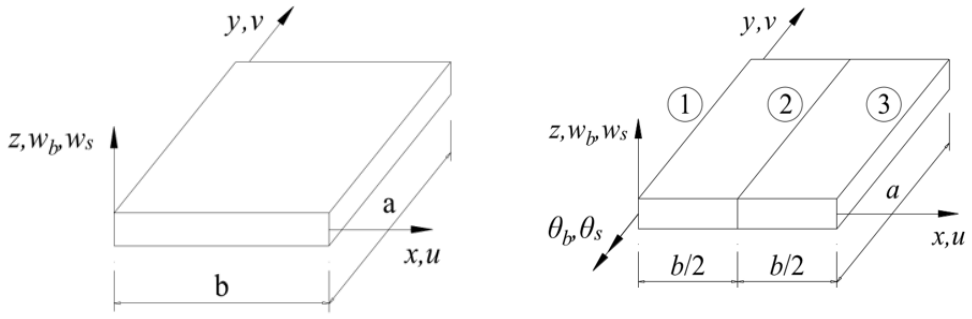

(a) Displacement field of RFSDT

(b) Displacement components of 3 nodal line FSM

Figure 1. Displacement components of a finite strip

2.2. *Formulation of stiffness matrix*

a. Interpolation functions

Fig. 1(b) illustrates a three-nodal-line finite strip with nodal lines 1, 2, and 3 of length a and width b. The displacement components u, v, w_b, and w_s correspond to the x-, y-, and z-directions, respectively. θ_b, θ_s, which are rotations about the y-direction, are represented by double-arrow notation. For a finite strip with simply supported at both ends, the displacement field can be expressed as follows:

$$u = \sum_{m=1}^{r}\sum_{i=1}^{k} N_{ui}u_i^m \sin(m\pi y/a); \quad v = \sum_{m=1}^{r}\sum_{i=1}^{k} N_{vi}v_i^m \cos(m\pi y/a)$$
$$w_b = \sum_{m=1}^{r}\sum_{i=1}^{k} N_{w_bi}w_{bi}^m \sin(m\pi y/a); \quad \theta_b = \sum_{m=1}^{r}\sum_{i=1}^{k} N_{\theta_bi}\theta_{bi}^m \sin(m\pi y/a) \tag{4}$$
$$w_s = \sum_{m=1}^{r}\sum_{i=1}^{k} N_{w_si}w_{si}^m \sin(m\pi y/a); \quad \theta_s = \sum_{m=1}^{r}\sum_{i=1}^{k} N_{\theta_si}\theta_{si}^m \sin(m\pi y/a)$$

The polynomial functions are adopted in the transverse direction, while trigonometric functions are selected in the longitudinal direction in order to satisfy the simply supported boundary conditions. Here, r denotes the number of series terms considered, and k represents the number of transverse interpolation functions.

For three-nodal-line finite strip, the transverse shape functions for the membrane components can be used according to Eq. (5), while those for the bending components are defined in accordance with Eq. (6):

$$\begin{aligned} N_{u1} &= N_{v1} = 1 - 3(x/b) + 2(x/b)^2 \\ N_{u2} &= N_{v2} = 4(x/b) - 4(x/b)^2 \\ N_{u3} &= N_{v3} = -(x/b) + 2(x/b)^2 \end{aligned} \tag{5}$$

$$\begin{aligned} N_{w_b1} &= N_{w_s1} = 1 - 23(x/b)^2 + 66(x/b)^3 - 68(x/b)^4 + 24(x/b)^5 \\ N_{\theta_b1} &= N_{\theta_s1} = x\left[1 - 6(x/b) + 13(x/b)^2 - 12(x/b)^3 + 4(x/b)^4\right] \\ N_{w_b2} &= N_{w_s2} = 16(x/b)^2 - 32(x/b)^3 + 16(x/b)^4 \\ N_{\theta_b2} &= N_{\theta_s2} = x\left[-8(x/b) + 32(x/b)^2 - 40(x/b)^3 + 16(x/b)^4\right] \\ N_{w_b3} &= N_{w_s3} = 7(x/b)^2 - 34(x/b)^3 + 52(x/b)^4 - 24(x/b)^5 \\ N_{\theta_b3} &= N_{\theta_s3} = x\left[-(x/b) + 5(x/b)^2 - 8(x/b)^3 + 4(x/b)^4\right] \end{aligned} \tag{6}$$

b. Stiffness matrix

The stiffness matrix of the finite strip is derived from the strain energy of the plate:

$$W = \frac{1}{2}\int_{\Omega} \{\varepsilon_p\}^T [D_p] \{\varepsilon_p\} d\Omega + \frac{\eta}{2}\int_{\Omega} \{\varepsilon_s\}^T [D_s] \{\varepsilon_s\} d\Omega \tag{7}$$

where η is shear corrective coefficient ($\eta = 5/6$). The strain components $\{\varepsilon_p\}$ and $\{\varepsilon_s\}$ are the in-plane and out-plane strains, respectively. These components are given as follows:

$$\{\varepsilon_p\}^T = \{\varepsilon_{xx} \quad \varepsilon_{yy} \quad \gamma_{xy}\} \tag{8}$$

$$\{\varepsilon_s\}^T = \{\gamma_{xz} \quad \gamma_{yz}\} \tag{9}$$

The elastic stiffness matrices are represented as follows:

$$[D_p] = \frac{E}{1-\nu^2}\begin{bmatrix} 1 & \nu & 0 \\ \nu & 1 & 0 \\ 0 & 0 & \dfrac{1-\nu}{2} \end{bmatrix} \tag{10}$$

$$[D_s] = \frac{E}{2(1+\nu)}\begin{bmatrix}1 & 0\\ 0 & 1\end{bmatrix} \tag{11}$$

The bending and shear strain components in Eqs. (8) and (9) are determined by replacing Eq. (4) into Eq. (3)

$$\{\varepsilon_p\} = \sum_{m=1}^{r}\sum_{i=1}^{k}\left[B_{pi}^{m}\right]\{\delta^m\} \tag{12}$$

$$\{\varepsilon_s\} = \sum_{m=1}^{r}\sum_{i=1}^{k}\left[B_{si}^{m}\right]\{\delta^m\} \tag{13}$$

where the matrices $\left[B_{pi}^{m}\right]$ and $\left[B_{si}^{m}\right]$ are expressed for the i-th transverse term and the m-th longitudinal series as follows:

$$\left[B_{pi}^{m}\right] = \begin{bmatrix} \dfrac{\partial N_{ui}}{\partial x}S & 0 & -z\dfrac{\partial^2 N_{w_b i}}{\partial x^2}S & -z\dfrac{\partial N_{\theta_b i}}{\partial x^2}S & 0 & 0\\ 0 & -N_{vi}\xi S & zN_{w_b i}\xi C & zN_{\theta_b i}\xi C & 0 & 0\\ N_{ui}\xi C & \dfrac{\partial N_{vi}}{\partial x}C & -2z\dfrac{\partial N_{w_b i}}{\partial x}\xi C & -2z\dfrac{\partial N_{\theta_b i}}{\partial x}\xi C & 0 & 0 \end{bmatrix} \tag{14}$$

$$\left[B_{si}^{m}\right] = \begin{bmatrix} 0 & 0 & 0 & 0 & \dfrac{\partial N_{w_s i}}{\partial x}S & \dfrac{\partial N_{\theta_s i}}{\partial x}S\\ 0 & 0 & 0 & 0 & N_{w_s i}\xi C & N_{\theta_s i}\xi C \end{bmatrix} \tag{15}$$

with $S = \sin(m\pi y/a)$, $C = \cos(m\pi y/a)$ and $\xi = m\pi/a$.

The displacement components of the i-th nodal line and the m-th serie are obtained as follows:

$$\left\{\delta_i^m\right\}^T = \left\{u_i^m \quad v_i^m \quad w_{bi}^m \quad \theta_{bi}^m \quad w_{si}^m \quad \theta_{si}^m\right\} \tag{16}$$

The strip stiffness matrix can be formulated by replacing Eqs. (12) and (13) into Eq. (7). for the finite strip with simply supported at both ends, the strip stiffness matrix contains r diagonal matrices and has the following form:

$$[K]_e = \begin{bmatrix} [K]_{e11} & 0 & \ldots & 0\\ 0 & [K]_{e22} & \ldots & 0\\ \ldots & \ldots & \ldots & \ldots\\ 0 & 0 & \ldots & [K]_{err} \end{bmatrix} \tag{17}$$

with:

$$[k]_{emm} = \int_{\Omega}\left[B_p^m\right]^T\left[D_p\right]\left[B_p^m\right]d\Omega + \eta\int_{\Omega}\left[B_s^m\right]^T[D_s]\left[B_s^m\right]d\Omega \tag{18}$$

The closed form of the stiffness matrix are presented in Appendix A.

c. Geometric stiffness matrix

The geometric stiffness matrix is derived from the work done by the in-plane normal stresses acting on the nonlinear strain components, as follows:

$$T = \frac{1}{2}\int_{\Omega}\left[T_1 - (T_1 - T_2)\frac{x}{b}\right]\left[\left(\frac{\partial u}{\partial y}\right)^2 + \left(\frac{\partial v}{\partial y}\right)^2 + \left(\frac{\partial w}{\partial y}\right)^2\right]d\Omega \tag{19}$$

where T_1 and T_2 denote the in-plane normal stress values at the i-th and j-th nodal lines, respectively. The geometric stiffness matrix is obtained by substituting Eq. (4) into Eq. (19). For a finite strip with simply supported at both ends, the geometric stiffness matrix takes the following form:

$$[K]_G = \begin{bmatrix} [K]_{G11} & 0 & ... & 0 \\ 0 & [K]_{G22} & ... & 0 \\ ... & ... & ... & ... \\ 0 & 0 & ... & [K]_{Grr} \end{bmatrix} \tag{20}$$

with

$$[k]_{Gmm} = \int_{\Omega} [G_m]^T [G_m] \left[T_1 - (T_1 - T_2) \frac{x}{b} \right] d\Omega \tag{21}$$

The closed-form expression of the geometric stiffness matrix is found in Appendix B.

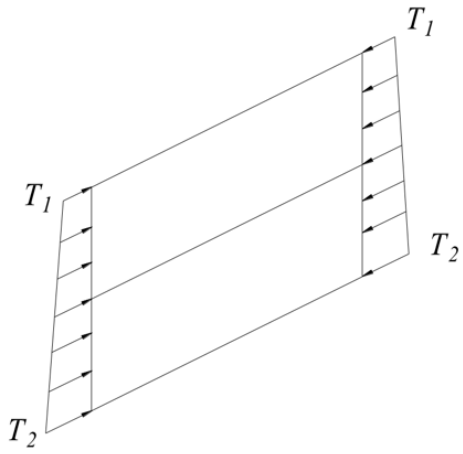

Figure 2. Normal stresses at both ends

The equations for solving the buckling problem of the plate is presented as follows:

$$[K]_e + \lambda [K]_G = 0 \tag{22}$$

where λ is the critical buckling load factor.

3. Convergence study

To verify the reliability of the proposed finite strip formulation, buckling analyses are performed for a square steel plate with all four edges simply supported and subjected to uniaxial compression and in-plane bending. The plate has a side length of 300 mm and a thickness of 3 mm. The material properties are taken as an elastic modulus of 210 GPa and a Poisson's ratio of 0.3. Table 1 presents the convergence study of the proposed finite strip model for the plate discretized using different numbers of strips, namely 1, 2, 3, 4, and 5 strips. It is observed that, for the plate subjected to in-plane bending, at least two strips are required to achieve convergence, whereas for the plate under uniaxial compression, a single strip is sufficient to satisfy the convergence criterion. The proposed model demonstrates faster convergence than those results in Ref. [26] (8 strips) and Ref. [13] (5 strips).

Table 1. Convergence study for buckling analysis of square plate: critical stress σ_{cr} (N/mm^2)

	Number of strips				
	1	2	3	4	5
Compression	75.877	75.865	75.865	75.865	75.865
Bending	22.834	22.386	22.383	22.382	22.382

4. Formulas for determining the critical buckling stress of plates

4.1. Exact solution for thin plates

A simply supported rectangular plate with edge lengths a and b is considered under two loading conditions: uniaxial compression (Fig. 3(a)) and in-plane bending (Fig. 3(b)). According to the exact solution for thin plates [31], the critical buckling stress is determined by the following expression:

$$\sigma_{cr} = k_\sigma \frac{\pi^2 E}{12\,(1-\nu^2)} \left(\frac{t}{b}\right)^2 \tag{23}$$

where E is elastic modulus, ν is Poisson's ratio, b is the width of plate and t is its thickness. k_σ is critical buckling coefficient. According to Ref. [41], the square plate ($a = b$) under uniaxial compression exhibits the minimum critical buckling stress corresponding to the buckling coefficient $k_\sigma = 4.0$. For the in-plane bending, the rectangular plate with an aspect ratio of $a = 2b/3$, with the corresponding critical buckling coefficient $k_\sigma = 23.9$.

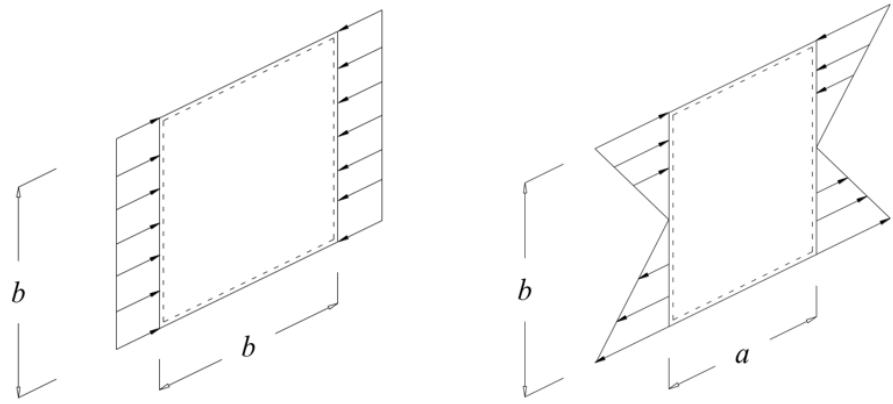

(a) Uniaxial compression (b) In-plane bending

Figure 3. Simply supported under uniaxial compression and in-plane bending

4.2. Critical buckling stress of thin and thick plates

In this sub-section, buckling analyses are conducted for a series of plates with different boundary conditions, including simply supported four edges, simply supported three edges and the remaining edge free, and two simply supported edges and the remaining edges clamped and free, respectively. The obtained results are compared with the exact solution for thin plates and with those reported in a previous publication.

Table 2 shows the buckling analysis results for both thin and thick plates under both uniaxial compression and in-plane bending with t/b ratios of 0.001, 0.005, 0.1, and 0.2, respectively. The

results obtained from the proposed finite strip are similar with the exact thin plate solution and with those reported in Ref. [13]. However, as the thickness of plate rises, the influence of shear deformation becomes significant, leading to a noticeable reduction in the critical buckling coefficient. Specifically, when the t/b ratio increases to 0.2, the discrepancy reaches approximately 28.0%. Clearly, the thin-plate results tend to overestimate the critical buckling stress of thick plate.

Table 2. Buckling coefficient of simply supported square plates

	t/b			
	0.001	0.05	0.1	0.2
Uniaxial compression				
Thin plate [41]	4.000	4.000	4.000	4.000
SAFSM [13]	3.999	3.929	3.737	3.126
FEM [34]	4.000	3.911	3.741	3.150
3D elastic [32]	4.000	3.911	3.741	3.150
Analytical [33]	–	3.944	3.786	3.264
Differential quadrature [35]	–	3.931	3.741	3.153
Present	4.001	3.929	3.732	3.126
In-plane bending				
Thin plate [41]	23.9	23.9	23.9	23.9
Present	23.886	23.875	20.212	14.149

Tables 3 and 4 present the buckling coefficients of plates subjected to uniaxial compression with various boundary conditions. The results indicate good agreement for thin plates, while the discrepancy increases as the plate thickness goes up.

Table 3. Buckling coefficient of square plates with two opposite edges simply supported and the remaining edges simply supported and free, respectively

	t/b	
	0.01	0.1
Thin plate [41]	1.440	1.440
SAFSM [13]	1.432	1.364
Present	1.434	1.379

Table 4. Buckling coefficient of square plates with two opposite edges simply supported and the remaining edges clamped and free, respectively

	t/b	
	0.01	0.1
Thin plate [41]	1.70	1.70
SAFSM [13]	1.70	1.59
Present	1.70	1.63

4.3. Influence of thickness on the critical buckling stress of plates

Buckling analyses are conducted for thin and thick isotropic simply supported plates with simply supported subjected to uniaxial compression and in-plane bending to investigate the influence of thickness on the critical buckling stress. The geometric dimension of the plate is characterized by a variable width-to-thickness ratios ranging from 8.0 to 100.

Fig. 4 illustrates the influence of thickness on the critical stress of the plates subjected to uniaxial compression and in-plane bending. The graph illustrates the relationship between the b/t ratio on the horizontal axis and the buckling coefficient $k_\sigma = \dfrac{12\sigma_{cr}\left(1-\nu^2\right)}{\pi^2 E}\left(\dfrac{b}{t}\right)^2$ on the vertical axis. It can be observed that a reduction in width-to-thickness ratio leads to a decrease in the critical buckling coefficient. When the b/t ratio is less than 20, the plate thickness exhibits a pronounced influence on the critical buckling coefficient. In contrast, when the ratio exceeds 40, the effect of thickness becomes negligible. In addition, the results increasingly converge to the exact thin plate solution as the b/t ratio becomes larger.

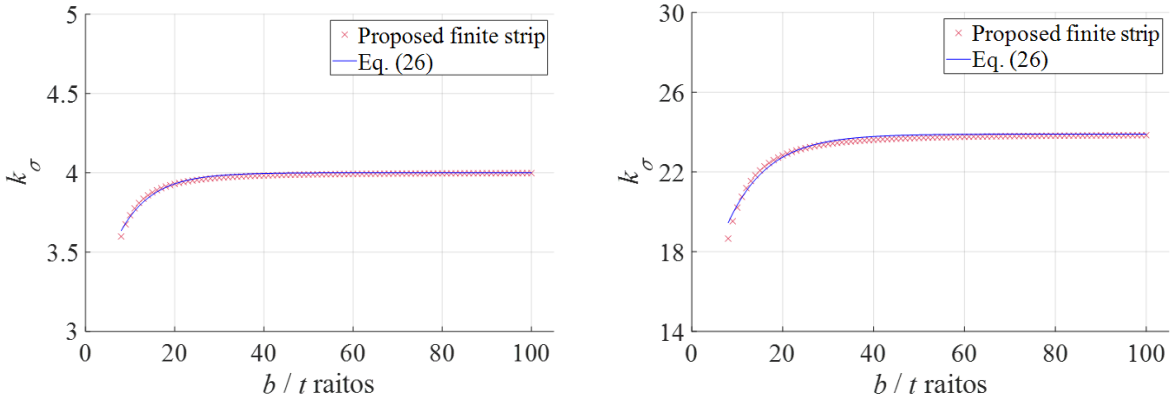

Figure 4. Influence of b/t ratios on critical buckling stress of plate

4.4. Approximate formulas for determining the critical buckling stress of plates

To the best of the authors' knowledge, the buckling behavior of isotropic simply supported plates subjected to uniaxial compression and in-plane bending has extensively investigated. However, approximate formulas for determining the critical buckling stress of thick plates under uniaxial compression and in-plane bending have not yet been provided. Therefore, approximate formulas for calculating the critical buckling stress of both thin and thick isotropic simply supported plates under uniaxial compression and in-plane bending are proposed to facilitate practical engineering calculations. Based on the results obtained from the buckling analyses of both thin and thick simply supported plates subjected to uniaxial compression and in-plane bending, a parametric study is utilized to propose formulas for determining the critical buckling stress for plates of both thin and thick configurations. From the relationship between the b/t ratios and the buckling coefficient, a formula in exponential form can be proposed as follows:

$$k_\sigma = a_1 + b_1 e^{c_1(b/t)} \tag{24}$$

where coefficients a_1, b_1, and c_1 are to be determined.

A parametric study is performed to determine the coefficients a_1, b_1, and c_1. These coefficients are found so as to satisfy the conditions of minimal coefficient of variation and maximal coefficient of determination. For the case of uniaxial compression, $a_1 = 4.0$, $b_1 = -1.10$, and $c_1 = -0.138$, whereas for the case of in-plane bending, $a_1 = 23.9$, $b_1 = -10.9$, and $c_1 = -0.112$, respectively. Eq. (24) can be reformulated for the uniaxial compression and in-plane bending, respectively, as Eqs. (25) and (26):

$$k_{\sigma,c} = 4.0 - 1.10e^{-0.138(b/t)} \tag{25}$$

$$k_{\sigma,b} = 23.9 - 10.9e^{-0.112(b/t)} \tag{26}$$

It should be noted that the proposed formulas are applicable to isotropic simply supported plates with a $8.0 \leq b/t \leq 100$. If the plate has a $b/t > 100$, the exact thin plate solution is applied to determine the critical buckling stress.

The comparison between the approximate formulas and the proposed finite strip method is presented in Table 5. It can be observed that when the plate is thin, i.e., when the b/t ratio is large, the buckling coefficient asymptotically approaches the value predicted by thin plate theory, namely 4.0 for the case of uniaxial compression and 23.9 for in-plane bending. The results obtained from the approximate formulas exhibit a high level of agreement with those predicted by the proposed finite strip method, as indicated by mean values (μ) close to unity. Both the plates under uniaxial compression and in-plane bending show low coefficients of variation (CoV). Specifically, the compressed plate has a CoV of 0.006 with a corresponding coefficient of determination $\left(R^2\right)$ of 0.9979, whereas the plate under bending presents a CoV of 0.017 and a R^2 of 0.9969.

Table 5. Statistical comparison of the approximate formulas with the proposed finite strip method

	Uniaxial compression			In-plane bending		
	μ	CoV	R^2	μ	CoV	R^2
Statistics values	1.002	0.006	0.9979	1.006	0.017	0.9969

4.5. Numerical applications

To verify the reliability of the approximate formulas, the critical buckling stress of the simply supported plates subjected to uniaxial compression and in-plane bending are determined using both the suggested formulas and the proposed finite strip method.

For the uniaxial compression, a square isotropic simply supported plate with side length $b = 100$ mm and thickness $t = 10$ mm is analyzed. For the in-plane bending, a rectangular plate with dimensions $a = 60$ mm, $b = 90$ mm, and $t = 10$ mm is examined. The plates are assumed to have Young's modulus of $E = 210$ GPa and a Poisson's ratio of $v = 0.3$. To determine the critical buckling stress using the approximate formulas, the procedure is conducted through the following steps:

In the first step, the buckling coefficient is determined using Eq. (25) for the plate under uniaxial compression and Eq. (26) for the plate subjected to in-plane bending. Subsequently, Eq. (23) is employed to calculate the critical buckling stress. Table 6 presents the calculation steps and the resulting critical buckling stresses of plates. The results demonstrate that the proposed formulas for determining the critical buckling stress of simply supported plates subjected to uniaxial compression and in-plane bending are highly reliable, with small discrepancy of only 2.0% for the in-plane bending case and 0.23% for the uniaxial compression situation.

Table 6. Critical buckling stress of plates under uniaxial compression and in-plane bending

	Uniaxial compression	In-plane bending
Buckling coefficient	$k_{\sigma,c} = 4.0 - 1.10e^{-0.138(100/10)}$	$k_{\sigma,b} = 23.9 - 10.9e^{-0.112(90/10)}$
	$k_{\sigma,c} = 3.7232$	$k_{\sigma,b} = 19.922$
σ_{cr}, approximate formula	$\sigma_{cr,c} = k_\sigma \frac{\pi^2 210000}{12(1-0.3^2)} \left(\frac{10}{100}\right)^2$	$\sigma_{cr,b} = k_\sigma \frac{\pi^2 210000}{12(1-0.3^2)} \left(\frac{10}{90}\right)^2$
	$\sigma_{cr,c} = 7066.8$ MPa	$\sigma_{cr,b} = 46681.4$ MPa
σ_{cr}, proposed FSM	$\sigma_{cr,c} = 7083.3$ MPa	$\sigma_{cr,b} = 45759.1$ MPa
Discrepancies	0.23%	2.00%

5. Conclusions

This paper further enhances the finite strip formulation based on the refined first-order shear deformation plate theory (RFSDT). The proposed model accounts for transverse shear deformation through the plate thickness and is capable of predicting the critical buckling stress of both thin and thick plates in close agreement with previously published results. In addition, the proposed finite strip exhibits very rapid convergence, as the convergence condition can be achieved even when the plate is discretized into a single strip. Explicit closed-form stiffness matrices are derived to improve computational efficiency and reduce resource requirements. Moreover, practical formulas for determining the critical buckling stress of simply supported plates under in-plane compression and bending are proposed through a parametric study. These formulas explicitly account for the influence of plate thickness on the critical buckling stress and demonstrate high reliability, as evidenced by low coefficients of variation and high coefficients of determination.

References

[1] Cheung, Y. K. (1976). *Finite Strip Method in Structural Analysis*. Pergamon Press, New York.

[2] Hancock, G. J. (1978). Local, distortional, and lateral buckling of I-beams. *Journal of the Structural Division*, 104(11):1787–1798.

[3] Tseng, Y.-P., Lee, C.-T. (1995). Bending analysis of bimodular laminates using a higher-order finite strip method. *Composite Structures*, 30:341–350.

[4] Ovesy, H. R., Ghannadpour, S. A. M., Zia-Dehkordi, E. (2013). Buckling analysis of moderately thick composite plates and plate structures using an exact finite strip. *Composite Structures*, 95:697–704.

[5] Dawe, D. J., Wang, S. (2000). Postbuckling analysis of composite laminated panels. *AIAA Journal*, 38 (11):2160–2170.

[6] Fazilati, J., Ovesy, H. R. (2010). Dynamic instability analysis of composite laminated thin-walled structures using two versions of FSM. *Composite Structures*, 92(9):2060–2065.

[7] Azhari, M. (1993). Local and post-local buckling of plates and plate assemblies using the finite strip method. PhD thesis, UNSW Sydney.

[8] Cheung, M. M., Song, Z. (2009). Finite-strip method for the analysis of cracked plates with application to plate-girder bridges. *Journal of Structural Engineering*, 135(2):198–205.

[9] Papangelis, J. P., Hancock, G. J. (1995). Computer analysis of thin-walled structural members. *Computers and Structures*, 56(1):157–176.

[10] Schafer, B. W., Adany, S. (2006). Buckling analysis of cold-formed steel members using CUFSM: conventional and constrained finite strip methods. In *18th International Specialty Conference on Cold-Formed Steel Structures*.

[11] Hancock, G. J., Pham, C. H. (2013). Shear buckling of channel sections with simply supported ends using the semi-analytical finite strip method. *Thin-Walled Structures*, 71:72–80.

[12] Hancock, G. J., Pham, C. H. (2015). Buckling analysis of thin-walled sections under localised loading using the semi-analytical finite strip method. *Thin-Walled Structures*, 86:35–46.
[13] Hinton, E. (1978). Buckling of initially stressed Mindlin plates using a finite strip method. *Computers & Structures*, 8(1):99–105.
[14] Bui, H. C., Rondal, J. (2008). Buckling analysis of thin-walled sections by semi-analytical Mindlin-Reissner finite strips: A treatment of drilling rotation problem. *Thin-Walled Structures*, 46(6):646–652.
[15] Feng, K., Xu, J. (2017). Buckling analysis of composite cylindrical shell panels by using Legendre polynomials hierarchical finite-strip method. *Journal of Engineering Mechanics*, 143(4).
[16] Zou, G., Qiao, P. (2002). Higher-order finite strip method for postbuckling analysis of imperfect composite plates. *Journal of Engineering Mechanics*, 128(9):1008–1015.
[17] Jafari, N., Azhari, M., Heidarpour, A. (2014). Local buckling of rectangular viscoelastic composite plates using finite strip method. *Mechanics of Advanced Materials and Structures*, 21(4):263–272.
[18] Mohajeri, S., Sarrami, S., Azhari, M., Naghsh, M. A. (2021). Dynamic instability, free vibration, and buckling analysis of MR fluid sandwich plates with FG face layers using the HSDT-based finite strip method. *Mechanics Based Design of Structures and Machines*, 51(8):4560–4587.
[19] Bui, H. C., Chiem, D. T. Q. (2026). Local buckling of thin- and thick-walled open sections using an enhanced Mindlin-Reissner finite strip with drilling degree of freedom. *International Journal of Structural Stability and Dynamics*.
[20] Bui, H. C., Chiem, D. T. Q. (2026). Local buckling analysis of thin- and thick-walled circular hollow sections under pure bending using third-order shear deformation finite strip with drilling degree of freedom. *Journal of Engineering Mechanics*, 152(8).
[21] Kim, S.-E., Thai, H.-T., Lee, J. (2009). Buckling analysis of plates using the two variable refined plate theory. *Thin-Walled Structures*, 47(4):455–462.
[22] Li, D., Deng, Z., Xiao, H. (2016). Thermomechanical bending analysis of functionally graded sandwich plates using four-variable refined plate theory. *Composites Part B: Engineering*, 106:107–119.
[23] Ahmed Houari, M. S., Benyoucef, S., Mechab, I., Tounsi, A., Adda Bedia, E. A. (2011). Two-variable refined plate theory for thermoelastic bending analysis of functionally graded sandwich plates. *Journal of Thermal Stresses*, 34(4):315–334.
[24] Mechab, I., Atmane, H. A., Tounsi, A., Belhadj, H. A., Bedia, E. A. A. (2010). A two variable refined plate theory for the bending analysis of functionally graded plates. *Acta Mechanica Sinica*, 26(6):941–949.
[25] Thai, H.-T., Kim, S.-E. (2010). Free vibration of laminated composite plates using two variable refined plate theory. *International Journal of Mechanical Sciences*, 52(4):626–633.
[26] Naghavi, M., Sarrami-Foroushani, S., Azhari, F. (2021). Bending analysis of functionally graded sandwich plates using the refined finite strip method. *Journal of Sandwich Structures & Materials*, 24(1):448–483.
[27] Mirzaei, S., Azhari, M., Bondarabady, H. A. R. (2014). On the use of finite strip method for buckling analysis of moderately thick plate by refined plate theory and using new types of functions. *Latin American Journal of Solids and Structures*, 12(3):561–582.
[28] Sarrami-Foroushani, S., Azhari, M. (2015). Nonlocal buckling and vibration analysis of thick rectangular nanoplates using finite strip method based on refined plate theory. *Acta Mechanica*, 227(3):721–742.
[29] Reddy, J. N. (2007). *Theory and Analysis of Elastic Plates and Shells*. CRC Press, Taylor & Francis Group.
[30] Thai, H.-T., Choi, D.-H. (2013). A simple first-order shear deformation theory for laminated composite plates. *Composite Structures*, 106:754–763.
[31] Timoshenko, S. P., Gere, J. M. (1961). *Theory of Elastic Stability*. McGraw-Hill, New York.
[32] Srinivas, S., Rao, A. K. (1969). Buckling of thick rectangular plates. *AIAA Journal*, 7(8):1645–1646.
[33] Reddy, J. N., Phan, N. D. (1985). Stability and vibration of isotropic, orthotropic and laminated plates according to a higher-order shear deformation theory. *Journal of Sound and Vibration*, 98(2):157–170.
[34] Rao, G., Venkataramana, J., Raju, K. (1975). Stability of moderately thick rectangular plates using a high precision triangular finite element. *Computers & Structures*, 5(4):257–259.

[35] Teo, T. M., Liew, K. M. (1999). A differential quadrature procedure for three-dimensional buckling analysis of rectangular plates. *International Journal of Solids and Structures*, 36(8):1149–1168.

[36] Hosseini-Hashemi, S., Atashipour, S. R., Fadaee, M. (2011). On the buckling analysis of isotropic, transversely isotropic, and laminated rectangular plates via Reddy plate theory: An exact closed-form procedure. *Proceedings of the Institution of Mechanical Engineers, Part C: Journal of Mechanical Engineering Science*, 226(5):1210–1224.

[37] Vieira, L., Gonçalves, R., Camotim, D. (2018). On the local buckling of RHS members under axial force and biaxial bending. *Thin-Walled Structures*, 129:10–19.

[38] Seif, M., Schafer, B. W. (2010). Local buckling of structural steel shapes. *Journal of Constructional Steel Research*, 66(10):1232–1247.

[39] Tu Quoc, C. D., Cuong, B. H., Duc, H. N. (2024). Formulas for determining the critical buckling stress of I-shaped members under pure bending. *Journal of Science and Technology in Civil Engineering (JSTCE) - HUCE*, 18(4).

[40] Cuong, B. H. (2021). Local buckling of thin-walled circular hollow section under uniform bending. *Journal of Science and Technology in Civil Engineering (STCE) - HUCE*, 15(4):88–98.

[41] Timoshenko, S. P., Gere, J. M. (1961). *Theory of Elastic Stability*. McGraw-Hill, New York.

Appendix A.

$$k_{11}=\frac{Ebtn^2(\nu-1)}{30a(\nu^2-1)}-\frac{7Eat}{6b(\nu^2-1)};\quad k_{12}=\frac{Etn(1-3\nu)}{8(\nu^2-1)};k_{17}=\frac{4Eat}{3b(\nu^2-1)}+\frac{Ebtn^2(\nu-1)}{60a(\nu^2-1)};\quad k_{18}=-\frac{nEt(1+\nu)}{6(\nu^2-1)};$$

$$k_{1-13}=-\frac{Eat}{6b(\nu^2-1)}-\frac{Ebtn^2(\nu-1)}{120a(\nu^2-1)};\quad k_{1-14}=\frac{Ent(1+\nu)}{24(\nu^2-1)};\quad k_{22}=-\frac{Ebtn^2}{15a(\nu^2-1)}-\frac{7Eat(1-\nu)}{12b(\nu^2-1)};\quad k_{27}=\frac{Ent(1+\nu)}{6(\nu^2-1)};$$

$$k_{28}=\frac{2Eat(1-\nu)}{3b(\nu^2-1)}-\frac{Ebtn^2}{30a(\nu^2-1)};\quad k_{2-13}=-\frac{Ent(1+\nu)}{24(\nu^2-1)};\quad k_{2-14}=\frac{Ebtn^2}{60a(\nu^2-1)}-\frac{Eat(1-\nu)}{12b(\nu^2-1)};$$

$$k_{33}=-\frac{1273Eat^3}{210b^3(\nu^2-1)}-\frac{139En^2t^3}{630ab(\nu^2-1)}-\frac{523En^4bt^3}{83160a^3(\nu^2-1)};\quad k_{34}=-\frac{569Eat^3}{420b^2(\nu^2-1)}-\frac{19En^4b^2t^3}{55440a^3(\nu^2-1)}-\frac{Et^3n^2(1155\nu+143)}{27720a(\nu^2-1)};$$

$$k_{39}=\frac{64Eat^3}{15b^3(\nu^2-1)}-\frac{En^4bt^3}{378a^3(\nu^2-1)}+\frac{64En^2t^3}{315ab(\nu^2-1)};\quad k_{3-10}=\frac{En^4b^2t^3}{2079a^3(\nu^2-1)}-\frac{2En^2t^3}{63a(\nu^2-1)}-\frac{16Eat^3}{7b^2(\nu^2-1)};$$

$$k_{3-15}=\frac{377Eat^3}{210b^3(\nu^2-1)}-\frac{131En^4bt^3}{166320a^3(\nu^2-1)}+\frac{11En^2t^3}{630ab(\nu^2-1)};\quad k_{3-16}=\frac{En^2t^3}{840a(\nu^2-1)}+\frac{29En^4b^2t^3}{332640a^3(\nu^2-1)}-\frac{121Eat^3}{420b^2(\nu^2-1)};$$

$$k_{44}=-\frac{Et^3\left(b^4n^4+154a^2b^2n^2+16434a^4\right)}{41580ba^3(\nu^2-1)};\quad k_{49}=\frac{16Eat^3}{15b^2(\nu^2-1)}-\frac{En^4b^2t^3}{3780a^3(\nu^2-1)}+\frac{2En^2t^3}{315a(\nu^2-1)};$$

$$k_{4-10}=\frac{En^2bt^3}{945a(\nu^2-1)}+\frac{En^4b^3t^3}{27720a^3(\nu^2-1)}-\frac{8Eat^3}{21b(\nu^2-1)};\quad k_{4-15}=\frac{121Eat^3}{420b^2(\nu^2-1)}-\frac{En^2t^3}{840a(\nu^2-1)}-\frac{29En^4b^2t^3}{332640a^3(\nu^2-1)};$$

$$k_{4-16}=\frac{Ebn^2t^3}{1512a(\nu^2-1)}+\frac{En^4b^3t^3}{110880a^3(\nu^2-1)}-\frac{19Eat^3}{420b(\nu^2-1)};\quad k_{55}=\frac{Et\left(523n^2b^2+9174a^2\right)}{16632ab(\nu+1)};\quad k_{56}=\frac{Et\left(19b^2n^2+143a^2\right)}{11088a(\nu+1)};$$

$$k_{5-11}=-\frac{Et\left(384a^2-10n^2b^2\right)}{756ab(\nu+1)};\quad k_{5-12}=\frac{5Et\left(33a^2-b^2n^2\right)}{2079a(\nu+1)};\quad k_{5-17}=-\frac{Et\left(1452a^2-131b^2n^2\right)}{33264ba(\nu+1)};\quad k_{5-18}=-\frac{Et\left(29b^2n^2+198a^2\right)}{66528a(\nu+1)};$$

$$k_{66}=\frac{Ebt\left(b^2n^2+77a^2\right)}{8316a(\nu+1)};\quad k_{6-11}=-\frac{Et\left(12a^2-b^2n^2\right)}{756a(\nu+1)};\quad k_{6-12}=-\frac{Etb\left(3b^2n^2+44a^2\right)}{16632a(\nu+1)};\quad k_{6-17}=\frac{Et\left(29b^2n^2+198a^2\right)}{66528a(\nu+1)};$$

$$k_{6-18}=-\frac{Ebt\left(3b^2n^2+110a^2\right)}{66528a(\nu+1)};\quad k_{77}=\frac{2Ebtn^2(\nu-1)}{15a(\nu^2-1)}-\frac{8Eat}{3b(\nu^2-1)};\quad k_{7-13}=\frac{4Eat}{3b(\nu^2-1)}+\frac{Ebtn^2(\nu-1)}{60a(\nu^2-1)};\quad k_{7-14}=-\frac{Ent(1+\nu)}{6(\nu^2-1)};$$

$$k_{88}=-\frac{4Ebtn^2}{15a(\nu^2-1)}-\frac{4Eat(1-\nu)}{3b(\nu^2-1)};\quad k_{8-13}=\frac{Etn(1+\nu)}{6(\nu^2-1)};\quad k_{8-14}=\frac{2Eat(1-\nu)}{3b(\nu^2-1)}-\frac{Ebtn^2}{30a(\nu^2-1)};$$

$$k_{99}=-\frac{128Eat^3}{15b^3(\nu^2-1)}-\frac{128En^2t^3}{315ab(\nu^2-1)}-\frac{16En^4bt^3}{945a^3(\nu^2-1)};\quad k_{9-15}=\frac{64Eat^3}{15b^3(\nu^2-1)}-\frac{Et^3n^4b}{378a^3(\nu^2-1)}+\frac{64Et^3n^2}{315ab(\nu^2-1)};$$

$$k_{9-16}=\frac{Et^3n^4b^2}{3780a^3(\nu^2-1)}-\frac{2Et^3n^2}{315a(\nu^2-1)}-\frac{16Eat^3}{15b^2(\nu^2-1)};\quad k_{10-10}=-\frac{32En^2bt^3}{945a(\nu^2-1)}-\frac{4En^4b^3t^3}{10395a^3(\nu^2-1)}-\frac{32Eat^3}{21b(\nu^2-1)};$$

$$k_{10-15}=\frac{16Eat^3}{7b^2(\nu^2-1)}-\frac{Et^3n^4b^2}{2079a^3(\nu^2-1)}+\frac{2Et^3n^2}{63a(\nu^2-1)};\quad k_{10-16}=\frac{Et^3n^2b}{945a(\nu^2-1)}+\frac{Et^3n^4b^3}{27720a^3(\nu^2-1)}-\frac{8Eat^3}{21b(\nu^2-1)};$$

$$k_{11-11}=\frac{16Et\left(n^2b^2+12a^2\right)}{189ab(\nu+1)};\quad k_{11-17}=-\frac{Et\left(192a^2-5n^2b^2\right)}{378ab(\nu+1)};\quad k_{11-18}=\frac{Et\left(12a^2-n^2b^2\right)}{756a(\nu+1)};\quad k_{12-12}=\frac{4Ebt\left(b^2n^2+44a^2\right)}{2079a(\nu+1)};$$

$$k_{12-17}=-\frac{5Et\left(33a^2-b^2n^2\right)}{2079a\left(\nu+1\right)};\quad k_{12-18}=-\frac{Etb\left(3b^2n^2+44a^2\right)}{16632a\left(\nu+1\right)};\quad k_{12-12}=\frac{4Ebt\left(b^2n^2+44a^2\right)}{2079a\left(\nu+1\right)};\quad k_{13-13}=\frac{Ebtn^2\left(\nu-1\right)}{30a\left(\nu^2-1\right)}-\frac{7Eat}{6b\left(\nu^2-1\right)};$$

$$k_{13-14}=-\frac{Etn\left(1-3\nu\right)}{8\left(\nu^2-1\right)};\quad k_{14-14}=-\frac{Ebtn^2}{15a\left(\nu^2-1\right)}-\frac{7Eat\left(1-\nu\right)}{12b\left(\nu^2-1\right)};\quad k_{15-15}=-\frac{1273Eat^3}{210b^3\left(\nu^2-1\right)}-\frac{139Et^3n^2}{630ab\left(\nu^2-1\right)}-\frac{523Et^3n^4b}{83160a^3\left(\nu^2-1\right)};$$

$$k_{15-16}=\frac{569Eat^3}{420b^2\left(\nu^2-1\right)}+\frac{19Et^3n^4b^2}{55440a^3\left(\nu^2-1\right)}+\frac{385Et^3\nu n^2}{9240a\left(\nu^2-1\right)}+\frac{143Et^3n^2}{27720a\left(\nu^2-1\right)};$$

$$k_{16-16}=-\frac{En^2bt^3}{270a\left(\nu^2-1\right)}-\frac{En^4b^3t^3}{41580a^3\left(\nu^2-1\right)}-\frac{83Eat^3}{210b\left(\nu^2-1\right)};$$

$$k_{17-17}=\frac{Et\left(523b^2n^2+9174a^2\right)}{16632ab\left(\nu+1\right)};\quad k_{17-18}=-\frac{Et\left(19b^2n^2+143a^2\right)}{11088a\left(\nu+1\right)};\quad k_{18-18}=\frac{Ebt\left(b^2n^2+77a^2\right)}{8316a\left(\nu+1\right)}$$

Appendix B.

$$k_{g11}=\frac{btn^2\left(7T_1+T_2\right)}{120a};\quad k_{g17}=\frac{T_1btn^2}{30a};\quad k_{g1-13}=-\frac{btn^2\left(T_1+T_2\right)}{120a};\quad k_{g22}=\frac{btn^2\left(7T_1+T_2\right)}{120a};\quad k_{g28}=\frac{T_1btn^2}{30a};$$

$$k_{g2-14}=-\frac{btn^2\left(T_1+T_2\right)}{120a};\quad k_{g33}=\frac{tn^2b\left(1407T_1+162T_2\right)}{20790a}+\frac{t^3n^2\left(7227T_1+1947T_2\right)}{83160ab}+\frac{t^3n^4b\left(469T_1+54T_2\right)}{83160a^3};$$

$$k_{g34}=\frac{b^2t^3n^4\left(97T_1+17T_2\right)}{332640a^3}+\frac{b^2tn^2\left(291T_1+51T_2\right)}{83160a}+\frac{t^3n^2\left(176T_1+253T_2\right)}{166320a};\quad k_{g35}=\frac{btn^2\left(469T_1+54T_2\right)}{6930a};$$

$$k_{g36}=\frac{b^2tn^2\left(97T_1+17T_2\right)}{27720a};\quad k_{g39}=\frac{b^2tn^2\left(45T_1+21T_2\right)}{2079ab}-\frac{t^3n^2\left(858T_1+198T_2\right)}{10395ab}+\frac{bt^3n^4\left(15T_1+7T_2\right)}{8316a^3};$$

$$k_{g3-10}=-\frac{b^2t^3n^4\left(37T_1+3T_2\right)}{83160a^3}+\frac{t^3n^2\left(253T_1+77T_2\right)}{20790a}-\frac{b^2tn^2\left(111T_1+9T_2\right)}{20790a};\quad k_{g3-11}=\frac{btn^2\left(15T_1+7T_2\right)}{693a};$$

$$k_{g3-12}=-\frac{b^2tn^2\left(37T_1+3T_2\right)}{6930a};\quad k_{g3-15}=\frac{131bt^3n^4\left(T_1+T_2\right)}{332640a^3}+\frac{tn^2\left(T_1+T_2\right)\left(393b^2-363t^2\right)}{83160ab};$$

$$k_{g3-16}=-\frac{b^2t^3n^4\left(17T_1+12T_2\right)}{332640a^3}-\frac{b^2tn^2\left(51T_1+36T_2\right)}{83160a}-\frac{t^3n^2\left(176T_2-77T_1\right)}{166320a};\quad k_{g3-17}=\frac{131btn^2\left(T_1+T_2\right)}{27720a};$$

$$k_{g3-18}=-\frac{b^2tn^2\left(17T_1+12T_2\right)}{27720a};\quad k_{g44}=\frac{t^3b^3n^4\left(13T_1+3T_2\right)}{665280a^3}+\frac{t^3bn^2\left(275T_1+33T_2\right)}{166320a}+\frac{b^3tn^2\left(13T_1+3T_2\right)}{55440a};$$

$$k_{g45}=\frac{b^2tn^2\left(97T_1+17T_2\right)}{27720a};\quad k_{g46}=\frac{b^3tn^2\left(13T_1+3T_2\right)}{55440a};\quad k_{g49}=\frac{b^2t^3n^4\left(7T_1+4T_2\right)}{41580a^3}+\frac{b^2tn^2\left(21T_1+12T_2\right)}{10395a}-\frac{t^3n^2\left(22T_1+11T_2\right)}{10395a};$$

$$k_{g4-10}=-\frac{bt^3n^2\left(3T_1-T_2\right)}{3780a}-\frac{T_1b^3t^3n^4}{27720a^3}-\frac{tn^2T_1b^3}{2310a};\quad k_{g4-11}=\frac{b^2tn^2\left(7T_1+4T_2\right)}{3465a};\quad k_{g4-12}=-\frac{T_1b^3tn^2}{2310a};$$

$$k_{g4-15}=\frac{b^2t^3n^4\left(12T_1+17T_2\right)}{332640a^3}+\frac{b^2tn^2\left(36T_1+51T_2\right)}{83160a}+\frac{t^3n^2\left(176T_1-77T_2\right)}{166320a};\quad k_{g4-16}=-\frac{\left(T_1+T_2\right)btn^2}{110880a}\left[6b^2+\frac{b^2t^2n^2}{2a^2}+\frac{55t^2}{3}\right];$$

$$k_{g4-17}=\frac{b^2tn^2\left(12T_1+17T_2\right)}{27720a};\quad k_{g4-18}=-\frac{b^3tn^2\left(T_1+T_2\right)}{18480a};\quad k_{g55}=\frac{btn^2\left(469T_1+54T_2\right)}{6930a};\quad k_{g56}=\frac{b^2tn^2\left(97T_1+17T_2\right)}{27720a};$$

$$k_{g59}=\frac{btn^2\left(15T_1+7T_2\right)}{693a};\quad k_{g5-10}=-\frac{b^2tn^2\left(37T_1+3T_2\right)}{6930a};\quad k_{g5-11}=\frac{btn^2\left(15T_1+7T_2\right)}{693a};\quad k_{g5-12}=-\frac{b^2tn^2\left(37T_1+3T_2\right)}{6930a};$$

$$k_{g5-15}=\frac{131btn^2\left(T_1+T_2\right)}{27720a};\quad k_{g5-16}=-\frac{b^2tn^2\left(17T_1+12T_2\right)}{27720a};\quad k_{g5-17}=\frac{131btn^2\left(T_1+T_2\right)}{27720a};\quad k_{g5-18}=-\frac{b^2tn^2\left(17T_1+12T_2\right)}{27720a};$$

$$k_{g66}=\frac{b^3tn^2\left(13T_1+3T_2\right)}{55440a};\quad k_{g69}=\frac{b^2tn^2\left(7T_1+4T_2\right)}{3465a};\quad k_{g6-10}=-\frac{T_1b^3tn^2}{2310a};\quad k_{g6-11}=\frac{b^2tn^2\left(7T_1+4T_2\right)}{3465a};\quad k_{g6-12}=-\frac{T_1b^3tn^2}{2310a};$$

$$k_{g6-15}=\frac{b^2tn^2\left(12T_1+17T_2\right)}{27720a};\quad k_{g6-16}=-\frac{b^3tn^2\left(T_1+T_2\right)}{18480a};\quad k_{g6-17}=\frac{b^2tn^2\left(12T_1+17T_2\right)}{27720a};\quad k_{g6-18}=-\frac{b^3tn^2\left(T_1+T_2\right)}{18480a};$$

$$k_{g6-18}=-\frac{b^3tn^2\left(T_1+T_2\right)}{18480a};\quad k_{g77}=\frac{2btn^2\left(T_1+T_2\right)}{15a};\quad k_{g7-13}=\frac{T_2btn^2}{30a};\quad k_{g88}=\frac{2btn^2\left(T_1+T_2\right)}{15a};\quad k_{g8-14}=\frac{T_2btn^2}{30a};$$

$$k_{g99}=\frac{\left(T_1+T_2\right)}{945a}\left[\frac{8bt^3n^4}{a^2}+\frac{4tn^2\left(24b^2+24t^2\right)}{b}\right];\quad k_{g9-10}=-\frac{4\left(T_1-T_2\right)tn^2}{10395a}\left[12b^2+22t^2+\frac{b^2t^2n^2}{a^2}\right];\quad k_{g9-11}=\frac{32btn^2\left(T_1+T_2\right)}{315a};$$

$$k_{g9-12}=-\frac{16b^2tn^2\left(T_1-T_2\right)}{3465a};\quad k_{g9-15}=\frac{b^2tn^2\left(21T_1+45T_2\right)}{2079ab}-\frac{t^3n^2\left(198T_1+858T_2\right)}{10395ab}+\frac{b^2t^3n^4\left(7T_1+15T_2\right)}{8316a^3b};$$

$$k_{g9-16}=-\frac{b^2t^3n^4\left(4T_1+7T_2\right)}{41580a^3}-\frac{b^2tn^2\left(12T_1+21T_2\right)}{10395a}+\frac{t^3n^2\left(11T_1+22T_2\right)}{10395a};\quad k_{g9-17}=\frac{btn^2\left(7T_1+15T_2\right)}{693a};$$

$$k_{g9-18}=-\frac{b^2tn^2\left(4T_1+7T_2\right)}{3465a};\quad k_{g10-10}=\frac{2btn^2\left(T_1+T_2\right)}{10395a}\left[12b^2+44t^2+\frac{b^2t^2n^2}{a^2}\right];\quad k_{g10-11}=-\frac{16b^2tn^2\left(T_1-T_2\right)}{3465a};$$

$$k_{g10-12}=\frac{8b^3tn^2\left(T_1+T_2\right)}{3465a};\quad k_{g10-15}=\frac{b^2t^3n^4\left(3T_1+37T_2\right)}{83160a^3}+\frac{b^2tn^2\left(9T_1+111T_2\right)}{20790a}-\frac{t^3n^2\left(77T_1+253T_2\right)}{20790a};$$

$$k_{g10-16} = -\frac{btn^2\left(18T_2b^2 + 33T_2t^2 - 11T_1t^2\right)}{41580a} - \frac{T_2b^3t^3n^4}{27720a^3}; \quad k_{g10-17} = \frac{b^2tn^2\left(3T_1 + 37T_2\right)}{6930a}; \quad k_{g10-18} = -\frac{T_2b^3tn^2}{2310a};$$

$$k_{g11-11} = \frac{32btn^2\left(T_1 + T_2\right)}{315a}; \quad k_{g11-12} = -\frac{16b^2tn^2\left(T_1 - T_2\right)}{3465a}; \quad k_{g11-15} = \frac{btn^2\left(7T_1 + 15T_2\right)}{693a}; \quad k_{g11-16} = -\frac{b^2tn^2\left(4T_1 + 7T_2\right)}{3465a};$$

$$k_{g11-17} = \frac{btn^2\left(7T_1 + 15T_2\right)}{693a}; \quad k_{g11-18} = -\frac{b^2tn^2\left(4T_1 + 7T_2\right)}{3465a}; \quad k_{g12-12} = \frac{8b^3tn^2\left(T_1 + T_2\right)}{3465a}; \quad k_{g12-15} = \frac{b^2tn^2\left(3T_1 + 37T_2\right)}{6930a};$$

$$k_{g12-16} = -\frac{T_2b^3tn^2}{2310a}; \quad k_{g12-17} = \frac{b^2tn^2\left(3T_1 + 37T_2\right)}{6930a}; \quad k_{g12-18} = -\frac{T_2b^3tn^2}{2310a}; \quad k_{g13-13} = \frac{btn^2\left(T_1 + 7T_2\right)}{120a};$$

$$k_{g14-14} = \frac{btn^2\left(T_1 + 7T_2\right)}{120a}; \quad k_{g15-15} = \frac{btn^2\left(162T_1 + 1407T_2\right)}{20790a} + \frac{t^3n^2\left(1947T_1 + 7227T_2\right)}{83160ab} + \frac{bt^3n^4\left(54T_1 + 469T_2\right)}{83160a^3};$$

$$k_{g15-16} = -\frac{b^2t^3n^4\left(17T_1 + 97T_2\right)}{332640a^3} - \frac{b^2tn^2\left(51T_1 + 291T_2\right)}{83160a} - \frac{t^3n^2\left(253T_1 + 176T_2\right)}{166320a}; \quad k_{g15-17} = \frac{btn^2\left(54T_1 + 469T_2\right)}{6930a};$$

$$k_{g15-18} = -\frac{b^2tn^2\left(17T_1 + 97T_2\right)}{27720a}; \quad k_{g16-16} = \frac{b^3t^3n^4\left(3T_1 + 13T_2\right)}{665280a^3} + \frac{b^3tn^2\left(3T_1 + 13T_2\right)}{55440a} + \frac{bt^3n^2\left(33T_1 + 275T_2\right)}{166320a};$$

$$k_{g16-17} = -\frac{b^2tn^2\left(17T_1 + 97T_2\right)}{27720a}; \quad k_{g16-18} = \frac{b^3tn^2\left(3T_1 + 13T_2\right)}{55440a}; \quad k_{g17-17} = \frac{btn^2\left(54T_1 + 469T_2\right)}{6930a};$$

$$k_{g17-18} = -\frac{b^2tn^2\left(17T_1 + 97T_2\right)}{27720a}; \quad k_{g18-18} = \frac{b^3tn^2\left(3T_1 + 13T_2\right)}{55440a}$$

with $n = \pi m$.